Kinetically Stable Anode Interface for Li_3YCl_6-Based All-Solid-State Lithium Batteries

Weixiao Ji[a,1], Dong Zheng [a,1], Xiaoxiao Zhang[a], Tianyao Ding[a], Deyang Qu[a,*]

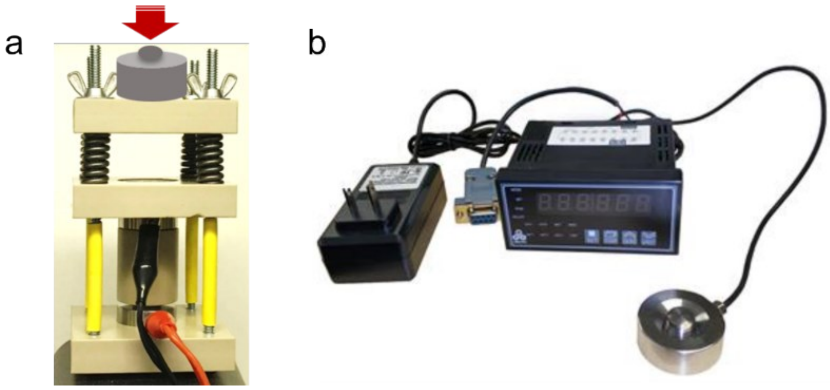

Fig. S1. a) Design of the solid-state cell used; b) picture of pressure calibration kit.

The cell is made of two stainless steel rods and a PEEK tube. A PEEK framework composed of three PEEK plates can allow the solid-state cell to have a constant pressure during testing. Four heavy duty springs allow for a gentle variation and a uniform distribution of pressure. A load cell was placed on top of the framework, in order to accurately measure the pressure to 1 kg during cell preparation process.

Fig. S2. Thickness measurement of a) LYCl pallet (100 mg), b) LYCl (100 mg)-LPSCl (25 mg) pallet, and c) cathode composite pallet (20 mg).

As shown in Fig. S2a, the LYCl electrolyte layer (100 mg) is 431 μm thick. As shown in Fig. S2b, the total thickness of LYCl electrolyte (100 mg) and LPSCl (25 mg) pallet is 495 μm. Therefore, the thickness of LPSCl interlayer is estimated to be 64 μm. As shown in Fig. S2c, the NCM-811 cathode composite layer (20 mg) is 133 μm thick.

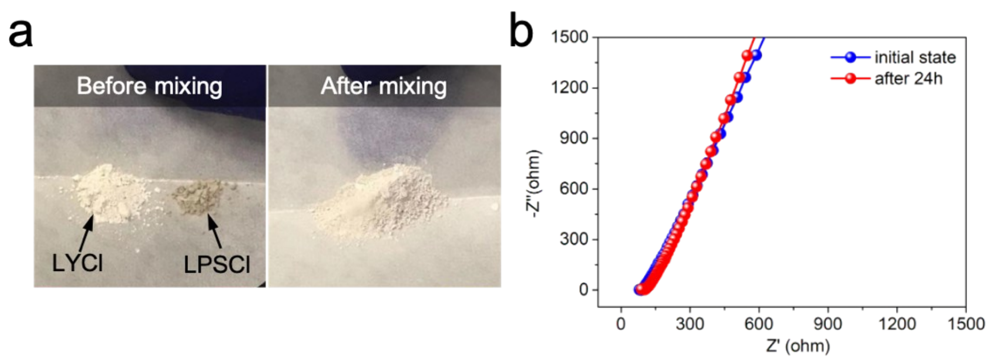

Fig. S3. a) Photographs of LPSCl and LYCl powder before and after grinding; b) ionic conductivity measurement of LPSCl-LYCl composite (20 wt.%: 100 wt.%) at room temperature.

The chemical compatibility between Li_6PS_5Cl and Li_3YCl_6 was investigated: 25 mg Li_6PS_5Cl and 100 mg Li_3YCl_6 was hand grounded in an agate mortar for 15 min until well mixed. The powder was then pressed into a pallet and hold at 370 MPa for 24 hours. The ionic conductivity was measured before and after 24 hours. As shown in Fig. S3b, the conductivity stays unchanged, representing the structure and transport behavior of the LPSCl-LYCl composite is barely changed. Therefore, a high chemical compatibility between Li_6PS_5Cl and $L_{i3}YCl_6$ can be expected.

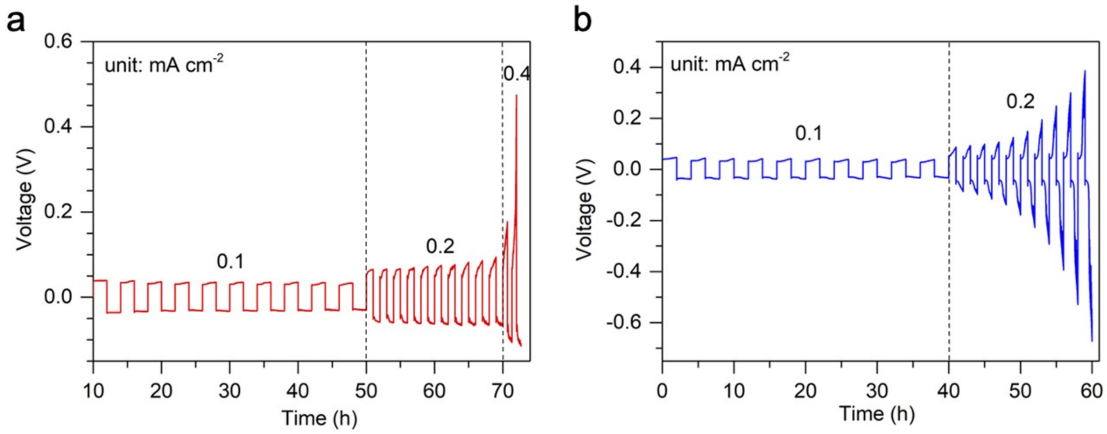

Fig. S4. Voltage profiles of Li/LPSCl/LYCl/LPSCl/Li symmetric cell cycled with a constant capacity of 0.2 mAh cm^{-2}: a) 15 mg and b) 10 mg LPSCl added on each side of LYCl pallet.

The thickness of interlayer was optimized by adding different amount of Li_6PS_5Cl powder: 10 mg, 15 mg, and 25 mg on each side of LYCl pallet. Fig. S4a (15 mg LPSCl) and Fig. S4b (10 mg LPSCl) exhibit an overpotential ramping up at 0.4 mA cm^{-2} and 0.2 mA cm^{-2}, respectively. By contrast, 25 mg LPSCl cell (Fig. 4b) demonstrate a maximum current density of 0.8 mA

cm^{-2}.

Table S1: Performance summary of the reported Li/Li symmetric cells based on halide electrolytes.

Halide-based symmetric cell	Stripping/plating current and capacity	Testing time	Polarization voltage	Ref.
$Li/Li_2Sr_{2/3}Cl_4/Li$	0.1 mA cm^{-2}, 0.1 mAh cm^{-2}	20 h	0.4 V	[1]
$Li/Li_3ScCl_6/Li$	0.1 mA cm^{-2}, 0.167 mAh cm^{-2}	2500 h	0.51 V	[2]
$Li/Li_3YBr_6/Li$	0.1 mA cm^{-2}, 0.1 mAh cm^{-2}	250 h	0.4 V	[3]
$Li/LPSCl/Li_3YCl_6/LPSCl/Li$	0.2 mA cm^{-2}, 0.2 mAh cm^{-2}	1000 h	0.1 V	**this work**

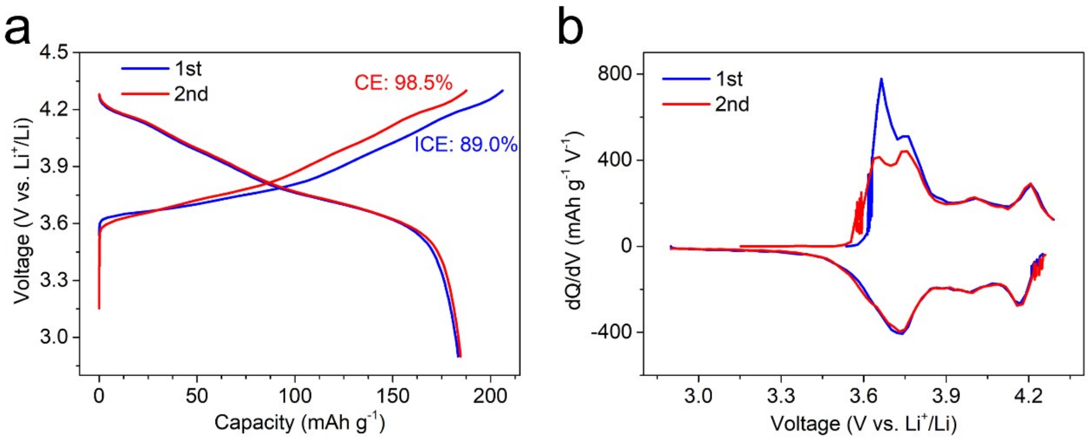

Fig. S5. a) Initial two charge/discharge profiles of NCM-811/LYCl/LPSCl/Li cell at 0.1 mA cm^{-2}; b) corresponding dQ/dV curves. The cathode composite is made of mixing NCM-811, LYCl, and conductive carbon at a weight ratio of 70:25:5.

Table S2: Summary of the reported cycling performance of sulfide- or halide-based full cells with high-Ni layered oxide cathodes.

Halide-based SE	Cathode	Anode	ICE	Cycle numbers, voltage range, capacity retention	Ref.
Li_3BrCl_6	NCM-811	In	69%	20 cycles, 2.5-4.4V, 7 %	[3]
Li_3InCl_6	NCM-811	Li-In	84%	70 cycles, 2.5-4.3V, good	[4]
Li_2ZrCl_6	$Li_{0.88}Co_{0.11}Al_{0.01}O_2$	Li-In	86%	100 cycles, 3.0-4.3V, 91%	[5]
Li_3YCl_6	NCM-811	Li	87%	100 cycles, 2.9-4.3V, 91%	**this work**
Sulfide-based SE					
$Li_{10}GeP_2S_{12}$	PEDOT coated NCM-811	Li-In	72%	77 cycles, 2.7-4.4V, 44%	[6]
Li_6PS_5Cl	$LiNbO_3$ coated NCA	Li	67%	100 cycles, 2.5-4.3V, 80.9%	[7]
Li_6PS_5Cl	$LiNi_{0.8}Mn_{0.05}Co_{0.15}O_2$	Li	64%	100 cycles, 2.8-4.25V, 74%	[8]
Li_6PS_5Cl	Li_2O-ZrO_2 coated high-Ni NMC	Ag-C	87%	1000 cycles, 2.5-4.25 V, 87%	[9]
β-Li_3PS_4	NCM-811	Li-In	71%	50 cycles, 2.7-4.3V, 69%	[10]
β-Li_3PS_4	NCM-811	Li-In	58%	25 cycles, 2.6-4.3V, 75%	[11]

Notes and references

1 L. Zhou, C.Y. Kwok, A. Shyamsunder, Q. Zhang, X. Wu, L.F. Nazar, *Energy & Environ. Sci.* 2020, **13**, 2056-2063.

2 J. Liang, X. Li, S. Wang, K.R. Adair, W. Li, Y. Zhao, C. Wang, Y. Hu, L. Zhang, S. Zhao, S. Lu, H. Huang, R. Li, Y. Mo, X. Sun, *J. Am. Chem. Soc.* 2020, **142**, 7012-7022.

3 C. Yu, Y. Li, K.R. Adair, W. Li, K. Goubitz, Y. Zhao, M.J. Willans, M.A. Thijs, C. Wang, F. Zhao, Q. Sun, S. Deng, J. Liang, X. Li, R. Li, T.-K. Sham, H. Huang, S. Lu, S. Zhao, L. Zhang, L. van Eijck, Y. Huang, X. Sun, *Nano Energy* 2020, **77**, 105097.

4 X. Li, J. Liang, N. Chen, J. Luo, K.R. Adair, C. Wang, M.N. Banis, T.-K. Sham, L. Zhang, S. Zhao, S. Lu, H. Huang, R. Li, X. Sun, *Angew. Chem. Int. Ed.* 2019, **58**, 16427-16432.

5 H. Kwak, D. Han, J. Lyoo, J. Park, S.H. Jung, Y. Han, G. Kwon, H. Kim, S.-T. Hong, K.-W. Nam, Y.S. Jung, *Adv. Energy Mater.* 2021, **11**, 2003190.

6 S. Deng, Y. Sun, X. Li, Z. Ren, J. Liang, K. Doyle-Davis, J. Liang, W. Li, M. Norouzi Banis, Q. Sun, R. Li, Y. Hu, H. Huang, L. Zhang, S. Lu, J. Luo, X. Sun, *ACS Energy Lett.* 2020, **5**, 1243-1251.

7 J.-M. Doux, H. Nguyen, D.H.S. Tan, A. Banerjee, X. Wang, E.A. Wu, C. Jo, H. Yang, Y.S. Meng, *Adv. Energy Mater.* 2020, **10**, 1903253.

8 S.H. Kim, K. Kim, H. Choi, D. Im, S. Heo, H.S. Choi, *J. Mater. Chem. A* 2019, **7**, 13650-13657.

9 Y.-G. Lee, S. Fujiki, C. Jung, N. Suzuki, N. Yashiro, R. Omoda, D.-S. Ko, T. Shiratsuchi, T. Sugimoto, S. Ryu, J.H. Ku, T. Watanabe, Y. Park, Y. Aihara, D. Im, I.T. Han, *Nature Energy* 2020, **5**, 299-308.

10 R. Koerver, I. Aygün, T. Leichtweiß, C. Dietrich, W. Zhang, J.O. Binder, P. Hartmann, W.G. Zeier, J. Janek, *Chem. Mater.* 2017, **29**, 5574-5582.

11 R. Koerver, F. Walther, I. Aygün, J. Sann, C. Dietrich, W.G. Zeier, J. Janek, *J. Mater. Chem. A* 2017, **5**, 22750-22760.